Tuning the superconducting state in the magnetic $MoSr_2YCu_2O_{8-\delta}$ materials

I. Felner and E. Galstyan
Racah Institute of Physics, The Hebrew University, Jerusalem 91904, Israel
(Received 31 July 2003; revised manuscript received 3 October 2003; published 15 January 2004)

The properties of $MoSr_2YCu_2O_{8-\delta}$ materials are found to systematically change with the oxygen concentration determined by the sintering and annealing conditions. The as-prepared (asp) sample is antiferromagnetically ordered at 16 K. The magnetic features are related to the Mo^{5+} sublattice. Annealing under an oxygen atmosphere induces superconductivity (SC) in the Cu-O planes, and the T_C and the shielding fraction values obtained depend strongly on the oxygen concentration. Annealing the asp material at 1030 °C under ambient oxygen atmosphere yields T_C of 18 K, whereas further annealing at 650 °C under 92 atm. of oxygen, shifts T_C to 32 K. The antiferromagnetic ordering, which coexists with SC state through effectively decoupled subsystems, is not affected by the presence or absence of the SC state. In all samples studied, $T_N < T_C$. This behavior resembles most of the inter-metallic magneto-superconductors, but is in sharp contrast to the isostructural $RuSr_2GdCu_2O_8$ system where $T_N > T_C$.

DOI: 10.1103/PhysRevB.69.024512 PACS number(s): 74.10.+v, 74.72.Jt, 74.25.Ha, 75.60.Ej

INTRODUCTION

The coexistence of weak ferromagnetism (W-FM) and superconductivity (SC) was discovered a few years ago in $RuSr_2Ln_{1.5}Ce_{0.5}Cu_2O_{10}$ (Ln=Eu and Gd, Ru-1222) layered cuprate systems,[1,2] and more recently in $RuSr_2GdCu_2O_8$ (Ru-1212).[3] Both Ru-based layered cuprate systems evolve from the $YBa_2Cu_3O_x$ structure where, the Ru ions reside in the Cu (1) site, and only one distinct Cu site [corresponding to Cu (2) in $YBa_2Cu_3O_x$] with fivefold pyramidal coordination, exists. The SC charge carriers originate from the CuO_2 planes and the W-FM state is confined to the Ru layers. In both systems, the magnetic order does not vanish and remains unchanged when SC sets in. Ru-1212 is SC around $T_C = 32$ K and displays a magnetic transition and at $T_M = 135$ K, thus $T_M/T_C \sim 4$. The Ru-1222 materials order magnetically at $T_M = 125-180$ K and show bulk SC below $T_C = 32-50$ K depending on the oxygen and/or Ce concentrations and on sample preparation.[4] The magnetic state of the Ru sublattice is not affected by the presence or absence of the SC state, indicating that the two states are practically decoupled.

Partial substitution of Mo for Cu(1) in the tetragonal $YBaSrCu_3O_x$ sample shows that the oxygen content is increased, and as a result T_C (81 K for un-doped material) is shifted to 86 K for 3 at % of Mo.[5] Recently we have noticed that the Ru ions in both Ru-1222 and Ru-1212 systems, can be replaced completely by Mo ions. The $MoSr_2R_{1.5}Ce_{0.5}Cu_2O_{10}$ (Mo-1222R) and $MoSr_2RCu_2O_8$ (Mo-1212R) systems can be obtained with most of the rare-earth (R) elements (Pr-Yb and Y) as nearly single-phase materials.[6,7] We have shown that in Mo-1212R, the magnetic and/or the SC states are determined mainly by the ionic radii of R.[7] For the light R ions (Pr and Nd) the materials are paramagnetic (PM) down to 4 K, whereas in the intermediate range (Sm-Tb), the Mo sublattice orders antiferromagnetically at T_N, ranging from 11 to 24 K. For the heavy R ions (Ho, Er, Tm, and Y), coexistence of SC and antiferromagnetism is observed. SC appears at T_C in the range 19–27 K and antiferromagnetism sets in at $T_N < T_C$. This is in contrast to the coexistence of SC and W-FM, observed in both Ru-1212 and Ru-1222 systems in which $T_M > T_C$.

Since Y ions are nonmagnetic, the study of $MoSr_2YCu_2O_{8-\delta}$ (Mo-1212Y) permits an easier direct interpretation of the SC and the intrinsic Mo antiferromagnetic (AFM) states. In this paper, we cover the physical properties of the system only. It is shown that sample prepared at ambient pressure is AFM at $T_N = 16$ K. The magnetic state is not affected by the presence or absence of the SC state. On the other hand, the SC state at T_C, 18–32 K, depends strongly on the oxygen concentration determined by the sintering and annealing conditions. Small differences of the annealing conditions are very important for the overall oxygen content and affect significantly the T_C and shielding fraction of the material.

EXPERIMENTAL DETAILS

Ceramic samples with a nominal composition of $MoSr_2YCu_2O_{8-\delta}$ were prepared by a solid-state reaction technique. Prescribed amounts of Y_2O_3, $SrCO_3$, Mo, and CuO were mixed and pressed into pellets and preheated at 750 °C for one day. The products were cooled, reground and sintered at elevated temperatures under various conditions. dc zero-field-cooled (ZFC) and field-cooled (FC) magnetic measurements in the range of 5–300 K were performed in a commercial (Quantum Design) superconducting quantum interference device (SQUID) magnetometer. The resistance was measured by a standard four contact probe and the ac susceptibility was measured by a homemade probe, with an excitation frequency and amplitude of 733 Hz and 30 mOe, respectively, both inserted in the SQUID magnetometer. The microstructure and the phase integrity of the materials were investigated by QUANTA (Fri Company) scanning electron microscopy (SEM) and by a Genesis energy depressive x-ray analysis (EDAX) device attached to the SEM.

EXPERIMENTAL RESULTS AND DISCUSSION

The $MoSr_2YCu_2O_{8-\delta}$ samples were sintered and annealed several times under various conditions (see below),

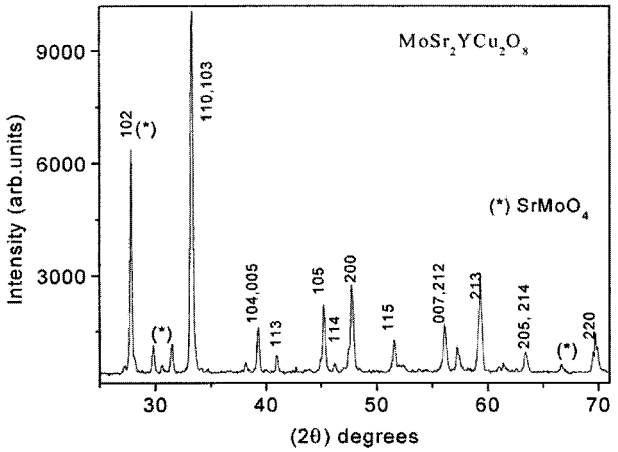

FIG. 1. The XRD pattern of $MoSr_2YCu_2O_{8-\delta}$ (sample C).

checked for phase purity and for the magnetic and SC properties. All studied materials were nearly single phase when sintered at least at 1030 °C. At lower temperatures multiphase materials are formed. The as-prepared (asp) non-SC sample was sintered at 1030 °C under ambient pressure. Sample B was first sintered at 950 °C for 24 h and then annealed at 1030 °C for 24 h under flowing oxygen. This sample shows a small fraction of the SC state at $T_C = 18$ K. Further annealing at 1030 °C under flowing oxygen for 24 h (sample C) increases the SC fraction. Sample D was obtained by further annealing under flowing oxygen of sample C at 600 °C for 48 h, and sample E is another piece of sample C which was annealed for 20 h under high oxygen pressure (92 atm) at 650 °C.

Powder x-ray diffraction (XRD) measurements indicate that all samples are nearly single-phase ($\sim$96%) materials and confirmed the tetragonal structure (space group P4/*mmm*). Due to incomplete reaction, all XRD patterns left a few minor reflections some of them belonging to the $SrMoO_4$ phase (Fig. 1). All attempts to completely get rid of them were unsuccessful. Least squares fits of the XRD patterns yield within the limit of uncertainty the same lattice parameters: $a = 3.811(1)$ Å and $c = 11.52(2)$ Å, for all samples studied. Due to these minor extra phases, the determination of the absolute oxygen content in the Mo-1212Y samples is difficult. Neutron diffraction studies are now carried on, in order to study the composition, as well as the detailed magnetic structure of these materials. In the next sections, assessments of the experimental results performed on the various samples are described.

A. Magnetic asp-$MoSr_2YCu_2O_{8-\delta}$ material

Figure 2 shows the ZFC and FC plots of the asp-Mo-1212Y sample measured at 40 Oe and 5 kOe. Apart from the magnetic irreversibility, the main effect to be seen is the peak obtained around 11(1) K in both branches indicating an antiferromagnetic ordering. The magnetic transition at $T_N = 16(1)$ K is defined as the merging temperature of the two curves (T_{irr}) when measured at low applied fields. T_{irr} is field dependent, and shifts with the applied field to lower temperatures, (inset of Fig. 2). Note that at 5 kOe, T_{irr} is below the

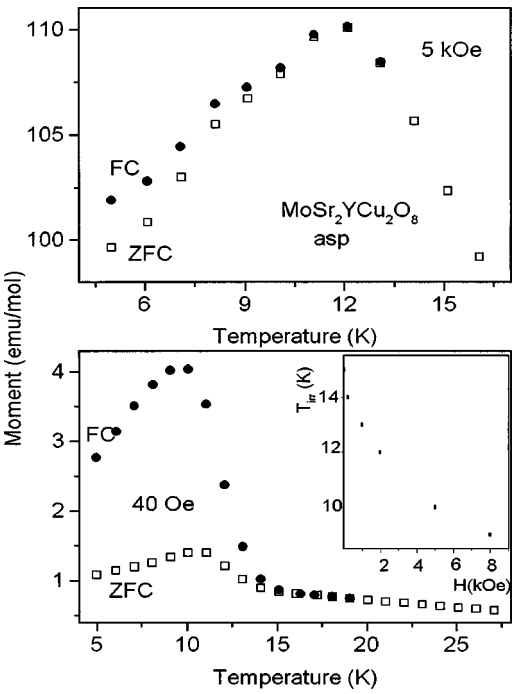

FIG. 2. ZFC and FC magnetization curves measured at 40 Oe and 5 kOe of the asp Mo-1212Y sample. The inset shows the field dependence of the irreversibility temperature.

peak position. Figure 1 shows the existence of the Pauli-paramagnetic $SrMoO_4$ phase[8] as an impurity phase. However, its small temperature independent susceptibility is negligible. It is also possible that small amount (not detected by XRD) of the W-FM Y_2CuO_4 (T_N 260 K) is also present. However this material reveals the magnetism of the CuO_2 sheets only when it is synthesized under high pressure.[9] Therefore, we may associate the AFM features shown in Fig. 2 with the Mo sublattice of the Mo-1212Y structure.

Isothermal M(H) measurements on the asp sample up to 50 kOe at various temperatures, have been carried out and the virgin curve obtained (at 5 K) is presented in Fig. 3. The linear M(H) curve up to about 15 kOe is typical of an AFM

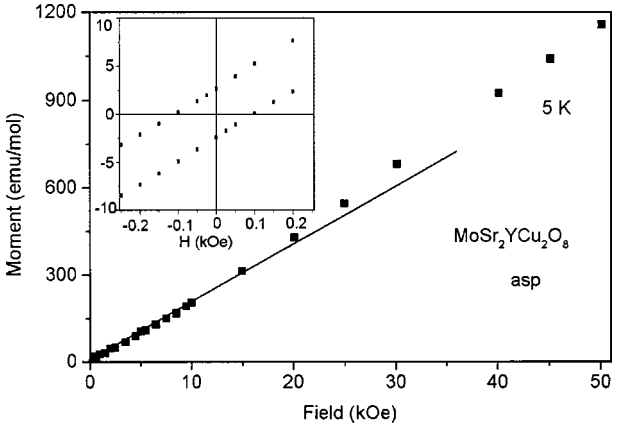

FIG. 3. The field dependence of the magnetization curves of the asp $MoSr_2YCu_2O_{8-\delta}$ sample measured at 5 K. The samll hysteresis loop at low fields is shown in the inset.

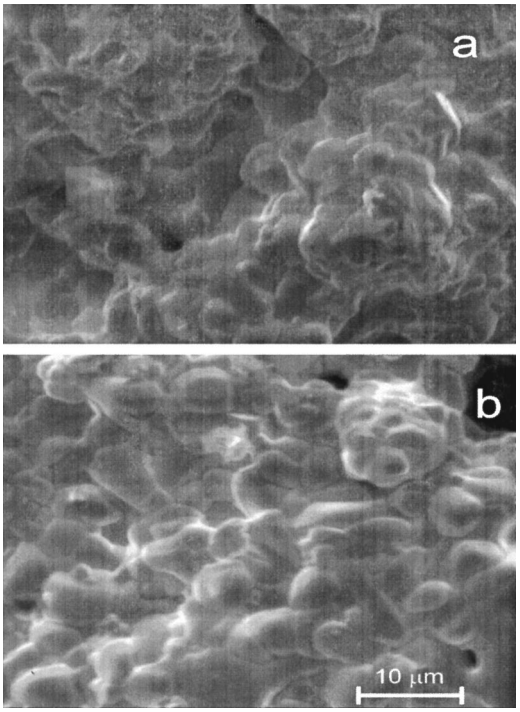

FIG. 4. SEM pictures of the asp (a) and (b) of sample C $MoSr_2YCu_2O_{8-\delta}$ materials.

substance. Above this field the slop changes slightly indicating a tiny canting of the Mo moments. This canting produces a small hysteresis loop (Fig. 3, inset) with a small remnant moment (2.7 emu/mol) and a coercive field of ~ 100 Oe. The surface morphology of the asp material [Fig. 4(a)], detected by SEM, shows that this sample has a granular structure with a typical grain size of 2–3 μm. However the grains are not well defined and isolated. We also observed a few separate spherical grains belong to the $SrMoO_4$ phase. The EDAX analysis confirms the initial stoichiometric composition of Mo:Sr:Y and Cu without any deficiency in the Mo content. The composition was found to be uniform from grain to grain.

B. SC and magnetic $MoSr_2YCu_2O_{8-\delta}$ samples

For samples annealed under oxygen flowing (at 1030 °C), in addition to the AFM order discussed above, a SC state (above $T_N = 16$ K) is induced. Figure 5 shows the ZFC and FC curves for sample B measured at 5 and 250 Oe. The negative signals in the ZFC curve and in the FC curve at 5 K clearly indicate a SC state with an onset at $T_C = 18$ (1) K, a value which was also confirmed by ac susceptibility and resistivity measurements. On the other hand, (i) the a pronounced peak at 11 K in both FC curves and (ii) the merging point of the ZFC and FC branches at $T_N = 16$ K (both similar to the asp sample) indicate the AFM ordering of the Mo sublattice. Note that (i) $T_N < T_C$ and (ii) the negative values in the FC curve at 5 Oe and around T_N. The shielding fraction (SF) deduced at 5 Oe is $\sim 4\%$ of the $-1/4\pi$ value, indicating that only a small fraction of the material becomes superconducting under these conditions. Scanning tunneling

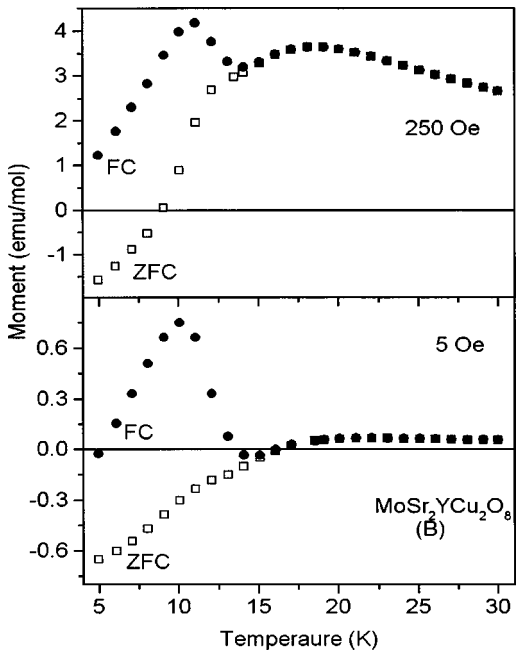

FIG. 5. ZFC and FC magnetization curves measured at 5 and 250 Oe for sample B ($T_C = 18$ K).

microscope measurements performed at 4.2 K on this sample show that some of the surface grains revealed gapless (nearly Ohmic) tunneling spectra, whereas for most of the grains, clear SC gaps were observed in the tunneling spectra.[7] The gap width exhibited spatial variations in the range 6–7 meV; thus the ratio $2\Delta/k_B T_C$ is around 6.8, within the range observed for various cuprate superconductors.[1,10] The gaps vanished at T_C and therefore are unambiguously associated with the SC state.

The ZFC and FC branches for sample C (annealed at 1030 °C for two days) are both negative below $T_C = 23$ K (Fig. 6), and the FC branch shows a clear peak at 11 K. The signature of bulk SC is the pronounced field expulsion (the Meissner effect), which appears in the FC curve. Without correcting for diamagnetism, the SF and the Meissner fractions (MFs) exceed 12% and 10%, respectively. This alone

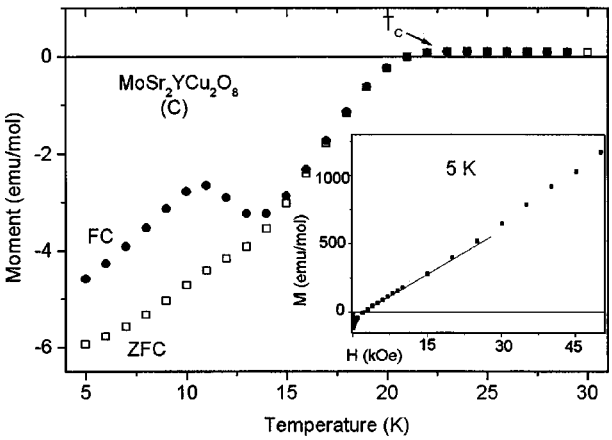

FIG. 6. ZFC and FC magnetization curves measured at 5 and 250 Oe and the M(H) plot at 5 K for sample C ($T_C = 22$ K).

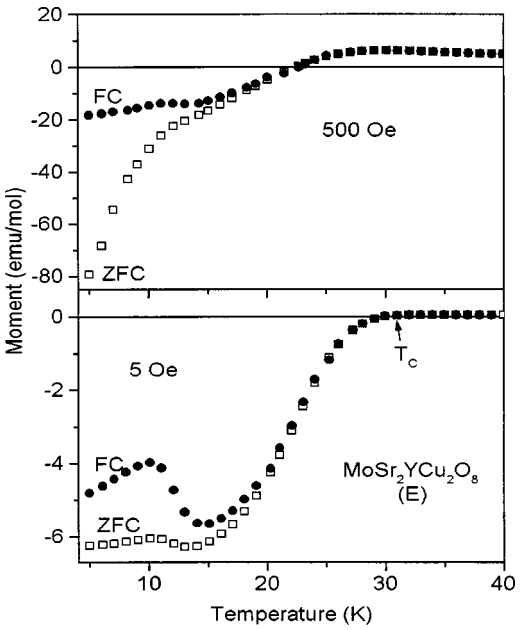

FIG. 7. ZFC and FC magnetization curves measured at 5 and 500 Oe sample E ($T_C = 32$ K).

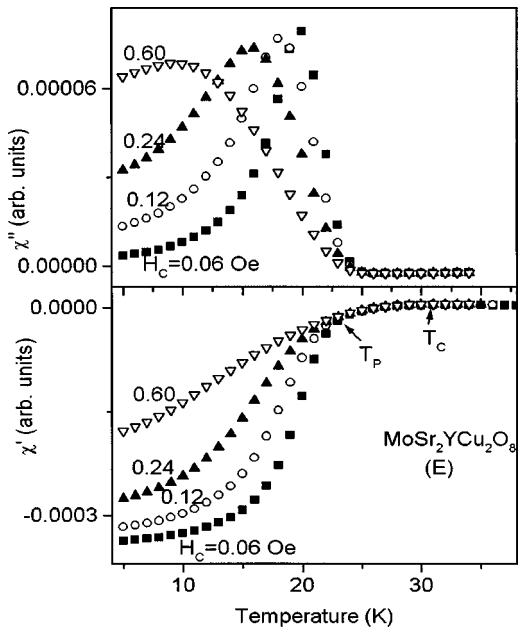

FIG. 8. The temperature dependence of the normalized real and imaginary ac susceptibility curves of sample E.

however, cannot be considered as indication for bulk superconductivity, although it would be very difficult to obtain such a signal by an impurity phase in a concentration not detectable with our XRD (Fig. 1). At high applied fields, the M(H) curve at 5 K (Fig. 6, inset) behaves similarly to that of the asp sample, indicating that the AFM state is not affected by the presence of the SC one. On the other hand, the morphology of sample C detected by SEM [Fig. 4(b)] is somewhat different from that of the non-SC (asp) sample. The grains are approximately spherical, with a typical size of 2–3 μm, and are well isolated from each other. Further annealing of sample C at 600 °C under flowing oxygen (sample D), shifts T_C to 26 K and increases the SF and MF to 23% and 18%, respectively (not shown). The relatively high MF value indicates a weak pinning of the expelled flux lines for this material.

C. High oxygen pressure annealed $MoSr_2YCu_2O_{8-\delta}$ sample

The ZFC and FC curves for sample E (annealed under 92-atm oxygen), measured at 5 and 500 Oe, are shown in Fig. 7. $T_C = 32$ K, obtained here, is a much higher than the 18 K for sample B, indicating that T_C depends only on the oxygen concentration. We tend to believe that annealing under higher oxygen pressure (not available in our laboratory) will shift T_C to even higher temperatures. Note (i) the peak around 11 K (at 5 Oe) in both branches and (ii) that the magnetic features are not visible in the 500-Oe curves in which the SC state is the dominant one. The SF and MF (at 5 K) are $\sim$23% and 18% of the $-1/4\pi$ value, the same values as for sample D ($T_C = 26$ K). We have not corrected for the demagnetization factor, which should be small, since the sample has a bar-shape form and the external field was parallel to the long axis. Therefore we may assume that these SF and MF values represent the bulk properties of the SC state which exists through the entire volume of the material. By the same token, the low SF and MF obtained may be the result of the grain size effect as follows. The penetration depth (λ) for the isostructure $RuSr_2GdCu_2O_8$ compound (with the same T_C) was evaluated to be around 10 μm.[11] Assuming a similar λ value for the isostructural $MoSr_2YCu_2O_{8-\delta}$, causes many grains with a size smaller than λ, not to expel the magnetic field and to reduce the diamagnetic signals in the ZFC and FC curves. Figure 8 exhibits the temperature dependence of the real $\chi'(T)$ and imaginary $\chi''(T)$ ac susceptibilities measured at various ac fields (H_{ac}). A similar behavior was obtained for Ru-1222.[12] It is readily observed that the broad transition for this granular superconductor occurs via two stages. The intragrain SC onset ($T_C = 32$ K), at which the grains become superconducting, is not affected by (H_{ac}). However, at $T_P = 24$ K, due to the weak-Josephson inter-grain coupling, both $\chi'(T)$ and $\chi''(T)$ are affected dramatically by H_{ac}. This behavior is typical for a granular superconductor with a weak intergrain coupling. Generally speaking, below T_P the susceptibility is governed mainly by the weak-link properties, whereas above T_P it is governed by the intragrain coupling.

With the purpose of acquiring information about the critical current density (J_C), we have measured the magnetic hysteresis (Fig. 9) of sample E at 5 K. Following Bean's approach, $J_C(H) = 30\,\Delta M/d$, where ΔM (in emu/cc) is the difference in M at the same H, and $d = 2.5$ μm (Fig. 4). J_C is obtained as $J_C = 1.8\times10^5$ and 1.0×10^5 A/cm^2 at values of $H = 0$ and 1000 Oe, respectively, which compare well with J_C obtained in Ru-1222 under the same conditions.[12] The linear field dependence of J_C on a semilogarithmic scale (with a slope of -0.66) is shown in Fig. 9 (inset).

Above T_C, the dc susceptibility curves at 10 kOe measured for all samples have the typical PM shape and adheres to the Curie-Weiss (CW) law: $\chi = \chi_0 + C/(T-\theta)$, where χ_0

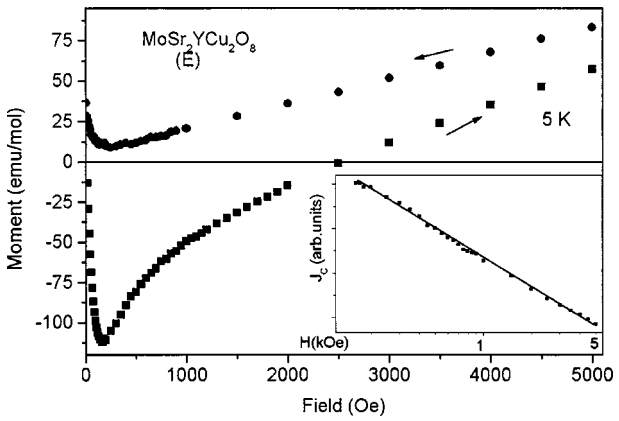

FIG. 9. The SC hysteresis low loop at 5 K and the field dependence of J_C in a semilogarithmic scale, for sample E.

is the temperature independent part of χ, C is the Curie constant, and θ is the CW temperature. Generally speaking, the PM values obtained for all samples are similar. The fits to the CW law yield $C=0.40-0.46$ emu K/mol Oe and a negative $\theta=$ from -7.6 to -2.2 K, which corresponds to an effective moment $P_{eff}=[1.79(2)-1.92(2)]\mu_B$. Note that neither the Y ions nor the Pauli paramagnetic $SrMoO_4$ phase contribute to C. Also the roughly temperature independent susceptibility of the Cu ions [$(1.8-2\times10^{-4}$ emu/mol Oe) (Ref. 13)] does not contribute to C. Therefore, the P_{eff} values obtained correspond to the Mo ions and are in good agreement with $1.73\mu_B$ expected for Mo^{5+} ($4d^1$, $S=0.5$). Therefore, we argue with high confidence that the prominent AFM features shown in this paper are related to the Mo^{5+} sublattice.

CONCLUSIONS

Synthetic conditions were optimized for Mo-1212Y, where the Mo sublattice is antiferromagnetically ordered at 16 K. The absolute value of the oxygen content of the samples is not known. The as-prepared sample is not superconducting. Superconductivity in the Cu-O layers is induced with an appropriate annealing which increase the oxygen concentration. The highest $T_C=32$ K was obtained by annealing under high oxygen pressure at 650 °C. It appears that small differences of the annealing conditions are very important for the overall oxygen content, and significantly affect T_C and the shielding fraction of the material. This finding is reminiscent of the typical behavior of the development of the SC in the well-known $YBa_2Cu_3O_x$ system. Neutron diffraction studies are now being carried on, in order to determine the detailed crystal and magnetic structures of the various compounds. The AFM ordering, which coexists with the superconducting state through effectively decoupled subsystems, is not affected by the presence or absence of the superconducting state. In all samples reported here, $T_C > T_N$. This rather surprising results raises a question as to why Mo-1212 behave so differently than the Ru-1212 system in which $T_C \ll T_N$. Further study is underway to determine this difference.

ACKNOWLEDGMENTS

This research was supported by the Israel Academy of Science and Technology and by the Klachky Foundation for Superconductivity.

[1] I. Felner, U. Asaf, Y. Levi, and O. Millo, Phys. Rev. B **55**, R3374 (1997); Physica C **334**, 141 (2000).
[2] Y.Y. Xue, B. Lorenz, A. Baikalov, D.H. Cao, Z.G. Li, and C.W. Chu, Phys. Rev. B **66**, 014503 (2002); **65**, 020511 (2002).
[3] C. Bernhard, J.L. Tallon, Ch. Niedermayer, Th. Blasius, A. Golnik, B. Btucher, R.K. Kremer, D.R. Noakes, C.E. Stronach, and E.J. Ansaldo, Phys. Rev. B **59**, 14099 (1999).
[4] I. Felner, U. Asaf, and E. Galstyan, Phys. Rev. B **66**, 024503 (2002).
[5] K. Rogacki, B. Dabrowski, O. Chmaissem, and J.D. Jorgensen, Phys. Rev. B **63**, 054501 (2001).
[6] I. Felner and E. Galstyan, Phys. Rev. B **68**, 064507 (2003).
[7] I. Felner, E. Galstyan, I. Asulin, A. Sharoni, and O. Millo (unpublished).
[8] S.I. Ikeda and N. Shirakawa, Physica C **341-348**, 785 (2000).
[9] H. Okada, M. Takano, and Y. Takeda, Phys. Rev. B **42**, 6831 (1990).
[10] H.L. Edwards *et al.*, Phys. Rev. Lett. **69**, 2967 (1992).
[11] Y.Y. Xue, B. Lorenz, R.L. Meng, A. Baikalov, and C.W. Chu, Physica C **364-365**, 251 (2001).
[12] I. Felner, E. Galstyan, B. Lorenz, D. Cao, Y.S. Wang, Y.Y. Xue, and C.W. Chu, Phys. Rev. B **67**, 134506 (2003).
[13] I. Felner, V.P.S. Awana, and E. Takayama-Muromachi, Phys. Rev. B **68**, 094508 (2003).